



Extraction and characterization of fiber from the flower stalk of the Agave plant for alternative reinforcing biocomposite materials

Imen Lalaymia^{1,2} · Ahmed Belaadi² · Azzeddeine Bedjaoui² · Hassan Alshahrani^{3,4} · Mohammad K. A. Khan^{3,4}

Received: 17 July 2023 / Revised: 7 August 2023 / Accepted: 20 August 2023
© The Author(s), under exclusive licence to Springer-Verlag GmbH Germany, part of Springer Nature 2023

Abstract

To achieve durability and biodegradability in the composite materials sector, natural fibers offer a preferable alternative to synthetic fibers. The morphological, physical, thermal, and mechanical features of the flower stalk fibers extracted from the *Agave americana* L. plant (FSAA) were investigated for the first time. Scanning electron microscopy and thermal analysis, Weibull distribution, Fourier transform infrared spectroscopy, and X-ray diffraction were all employed in the investigation. According to an XRD examination, the (FSAA) fibers contained crystallites that were 2.53 nm in size and had a crystallinity index of 29.15%. While the fibers' average strength in tension was $(64.34 \pm 11.43 \text{ MPa})$, their modulus of Young was $(77.61 \pm 15.90 \text{ GPa})$ and their strain at failure was $(1.5 \pm 0.31\%)$, their distribution required statistical Weibull analysis with two parameters (ML technique) to be performed. The findings of the thermal investigation carried out by TGA demonstrate that the fibers of (FSAA) exhibit thermal stability up to 339.57 °C and energy of kinetic activation of 68.1 kJ/mol. The significance of this research highlights the possible uses of this fiber in the field of biocomposites for industrial use such as construction, aerospace, and automotive industry.

Keywords Flower stalk of *Agave americana* · Thermophysical characterization · Mechanical test · Natural fiber · SEM observation

Highlights

- The first investigation of fiber properties extracted from flower stalks of *Agave americana*.
- The FSAA fibers are extracted using the water-retting method.
- Using the peak deconvolution technique, a crystallinity index of 29.15% was found.
- The average tensile strength and Young's modulus of the FSAA fibers are 64.34 MPa and 77.61 GPa, respectively.

✉ Ahmed Belaadi
a.belaadi@univ-skikda.dz; ahmedbelaadi1@yahoo.fr

- ¹ Department of Mechanical Engineering, Faculty of Technology, University 20 August 1955-Skikda, El-Hadaiek Skikda, Algeria
- ² Laboratory LGMM, University 20 August 1955- Skikda, El-Hadaiek Skikda, Algeria
- ³ Department of Mechanical Engineering, College of Engineering, Najran University, Najran, Saudi Arabia
- ⁴ Scientific and Engineering Research Centre, Deanship of Scientific Research, Najran University, Najran, Saudi Arabia

1 Introduction

Over the past few decades, natural fibers have attracted the interest of numerous researchers in a variety of industries, including textile, furniture, packaging, recreation, automotive, sports, construction, electronics, decorating, aerospace, kitchenware products, and others [1]. Natural fibers have many benefits over synthetic fibers, including biodegradability, accessibility, low density, non-toxicity, lightweight, reasonably priced, great thermal characteristics, and reduced equipment wear [2]. Due to their environment-friendly production and consumption practices, recycling capabilities, and value addition in the circular economy [3], natural fibers played an increasingly significant role in the biocomposite manufacturing and packaging sectors [4]. Glass, carbon, ceramic, and aramid synthetic fibers are particularly pricey, toxic, and unsustainable; they also pose concerns to human health when exposed for an extended period of time [5]. Natural fibers are predominantly derived from cellulose-rich plants, such as hemp [6], jute [7], kenaf [8], and banana pseudo-stem fiber [9]. The fact that these natural fibers are less costly,

widely accessible, produced with renewable resources, and possess a high specific strength gives them an edge over glass fibers [10, 11]. Cellulose, among natural polymers, is by far the most common. Nature produces over 10^{10} cellulose annually, which doubles the amount of biomass on Earth. Cellulose is a linear homopolymer composed of glucose residues in a D configuration with glycosidic bonds in the β -(1–4) position [12, 13]. Cellulosic natural fibers can be extracted from various sources, including higher plants such as algae. These fibers can also be obtained from plant fruits, seeds, stalks, and leaves. They consist mainly of cellulose, lignin, pectin, and hemicellulose wax [14]. The most typical process for removing premium fibers is water retting. The presence of bacteria and moisture during the retting process enables the breakdown of the plant's cellular tissues and the degradation of pectins, waxes, and other adhesive substances around the fibers, facilitating the splitting apart of individual fibers [15]. Cellulose remains the most abundant and important natural material due to its exceptional mechanical strength, making it suitable for a diverse array of applications. This has inspired researchers to look into novel fibers that could strengthen polymers and potential substitute dangerous man-made synthetic fibers [16]. According to Marcelet et al.'s morphological study of *Ficus religiosa* root fiber using electronic scanning microscopy, they found that the raw surface of the fiber was semi-lisse and consists of cellulose content, cire, and hemicellulose in significant percentages [17]. Kathirselvam et al. conducted an investigation on fibers from *Thespesia populnea* (TP) that has been exposed to various sodium hydroxide (NaOH) solution concentrations for varying lengths of time. In particular, measurements were done and reports were written about elements like the percentage of cellulose, crystallinity, thermal stability, tensile strength, and surface shape [18]. A study was carried out by Dao Cheng et al. to investigate the potential of natural *Luffa vine* (LV) fiber as a cellulose reinforcement for light, decay-resistant composite materials. The investigation examined the microstructure, as well as the morphological, thermal, chemical, and physical characteristics of the LV fiber. According to the results, the LV presents itself as a lightweight natural fiber with a porous structure and is distinguished by its low density, distinctive microscopic characteristics, and outstanding mechanical strength [19]. Babu et al. conducted a comprehensive analysis of an original natural fiber obtained from *Phaseolus vulgaris* (PVF). The presence of cellulose, which has a 43.01% crystallinity index, was eventually shown by PVFs' XRD analyses. The PVFs' surface morphology was investigated using various magnification levels, revealing the presence of cell formations with tiny voids on one side of the fiber. In contrast, the opposing side appeared smooth, indicating the presence of microfibrils [20]. The application of

natural fiber composites is frequently constrained by their susceptibility to elements like acidic/alkaline agents, moisture absorption, high temperatures, and salty conditions. Therefore, in order to speed up the development of viable products for both industrial and societal usage, researchers are anxious to examine the robustness of biofiber composites. In this regard, a recent investigation was carried out by Kumar et al. on a newly discovered natural fiber that was taken from the stems of the *Myriostachya wightiana* (MW) plant. This perennial grass, also known as Nalia grass in Odisha, India, is widely distributed in Bangladesh, Myanmar, Malaysia. Although MW stems are often used by artisans to make baskets, toys, ropes, and different storage bags, there has not been much substantial scientific research on MW fiber until this study. The study found that this grass contains a higher percentage of cellulose than other natural fibers, suggesting potential use in the paper and packaging industries as well as for cellulose nanofiber producers to create useful goods. This fiber can also be used in lightweight structural applications like composites due to its low density and strong strength [21]. Maran et al. conducted an analysis to explore the prospective application of freshly isolated cellulosic fibers from the *Sida mysorensis* plant in polymer composites as reinforcement. FTIR spectroscopy was employed to identify the various functional groups of SMF. *Sida mysorensis* fiber is the ideal material to replace the synthetic fibers in the fiber-reinforced plastics, according to all the aforementioned findings [22]. A research by Mansouri et al. completed a study on the burying *Agave americana* leaves in the soil to extract buried fibers (BF) as a composite polymer reinforcement. The findings revealed that lignin, hemicelluloses, and cellulose were the primary constituents of these buried fibers (BF). This study set out to investigate an innovative technique for removing buried fiber (BF) from the *Agave americana* L. plant. The obtained fibers underwent chemical, ATR-FTIR, XRD, SEM, and thermal tests after being buried with the plant leaves in the soil. According to the findings, BF extraction using a soil burying strategy could be effective and profitable. It was discovered to enhance the extracted fibers' quality, making them ideal for polymer composite reinforcement [23]. A study on fibers taken from the prop root of *Fragrant screw pine* (FSP) plant's prop root was done by Gerald et al. They discovered that alkali treatment considerably improved the hydrophobic and surface properties of these *Fragrant screw pine* root fibers (FSPRFs). The research team thoroughly characterized the alkali-treated FSPRFs (AFSPRFs), examining their mechanical, thermal, and chemical characteristics in order to foresee their possible use as reinforcement in polymer composites. The functional group, crystal structure, and surface characteristics of the fiber were determined by the team using Fourier

transform infrared spectroscopy (FTIR), X-ray diffraction (XRD), and scanning electron microscopy (SEM). Their research suggested that adding AFSPRFs as reinforcement to polymer composites could significantly enhance the thermomechanical characteristics of bio-based polymer matrix composites [24].

The succulent *Agave americana*, which is indigenous to Mexico but is produced all over the world, including the semi-arid and arid Ain Achir region of Annaba, Algeria, shows great promise for sustainable material development. The *Agave* plant is a separate species of the Agavaceae family and the Agavoideae subfamily. Its distinctive characteristics are its sturdy, elongated flower stalk, which may soar to a dizzying height of 30 feet and support clusters of vivid yellow or greenish-yellow blossoms. It should be noted that the plant dies after producing its blooms, leaving behind the sturdy stalk, which is frequently thrown away. This quality raises the *Agave*'s significance as a source for the creation of natural fabric. These stalks are the subject of our study because they are renowned for their toughness, which encourages effective resource usage. We encourage sustainability and help to lessen our impact on the environment by reusing this otherwise useless part of the plant. These flower stalks' strong, biodegradable fibers can be used as a beneficial alternative to synthetic fibers in the production of composite materials. The *Agave* plant's significance goes beyond its inherent toughness; it has the ability to transform industries looking for sustainable substitutes, signaling a movement in material science towards environmental consciousness.

Agave americana fibers were also known as Ramban [25], *Agave* fiber-reinforced biocomposites were green materials that had already been reprocessed, and employed in the automotive industry [26] and other industries like epoxy [27], epoxy, and matrix [28], biopolymer [29]. *Agave* fibers, on the other hand, had good mechanical qualities, such as strong toughness, robust adhesion to the fiber matrix, and minimal damageability [30].

This work offers a fresh investigation of the underutilized and abandoned resource of the *Agave* plant's flower stalk for fiber extraction and characterization in biocomposites. By filling a research void, it enhances understanding of environmentally friendly materials alternatives, specifically the potential of *agave* fiber to replace traditional synthetic materials, this study seeks to show a unique fiber that had been recovered from the flower stalk of *Agave americana* (FSAA), in contrast to previous studies that had explored fibers taken from the leaves and skin of leaves and others parts of *Agave americana*. Reinforcing bio-composite materials with (FSAA) fibers had never been described before. The crystallographic, thermal, mechanical, morphological, and physicochemical properties were evaluated using Fourier-transform infrared spectroscopy, scanning electron microscopy (SEM), thermogravimetric analysis (TGA and DSC), single fiber stress testing, and X-ray diffraction (XRD).

2 Materials and methods

2.1 Extraction of fibers

After peeling, the flower stalks of *Agave americana* (FSAA) (Fig. 1a) were cut into 50-cm (Fig. 1c, b) lengths and soaked in water (Fig. 1d) for 30–45 days at 30–35 °C to remove the fibers (Fig. 1e). The biological breakdown of the flower stem is sped up considerably by the anaerobic bacterial activity and in the process, allowing for fiber extraction. Fibers were separated from their stems by hand harvesting, washing, and air drying as shown in (Fig. 1f).

2.2 Characterization of the flower stalk of *Agave americana* fibers

2.2.1 Determination of density

The pycnometer method was widely used to determine how dense natural fibers are. It involved measuring the volume of submerged fibers using a water-filled container with a known volume. Pycnometer was the accepted practice when using the mass difference method to calculate the density of natural fibers. Density analysis was performed using liquid acetone, with a known density of (0.790 to 0.792 g/cm³) at normal temperature. Short segments of the natural fibers were separated and put inside a pycnometer with a volume of 25 ml ($V_{py}=25$ ml). The pycnometer's initial weight was noted as m_1 , while the weight following the addition of the fibers was noted as m_2 . Consequently, m_3 represents the weight of the FSAA fibers when combined with acetone. The evaluation was conducted five times, and the average value of each repetition was recorded as the density of the FSAA fibers, then Eq. (1) was used to obtain the density [31]:

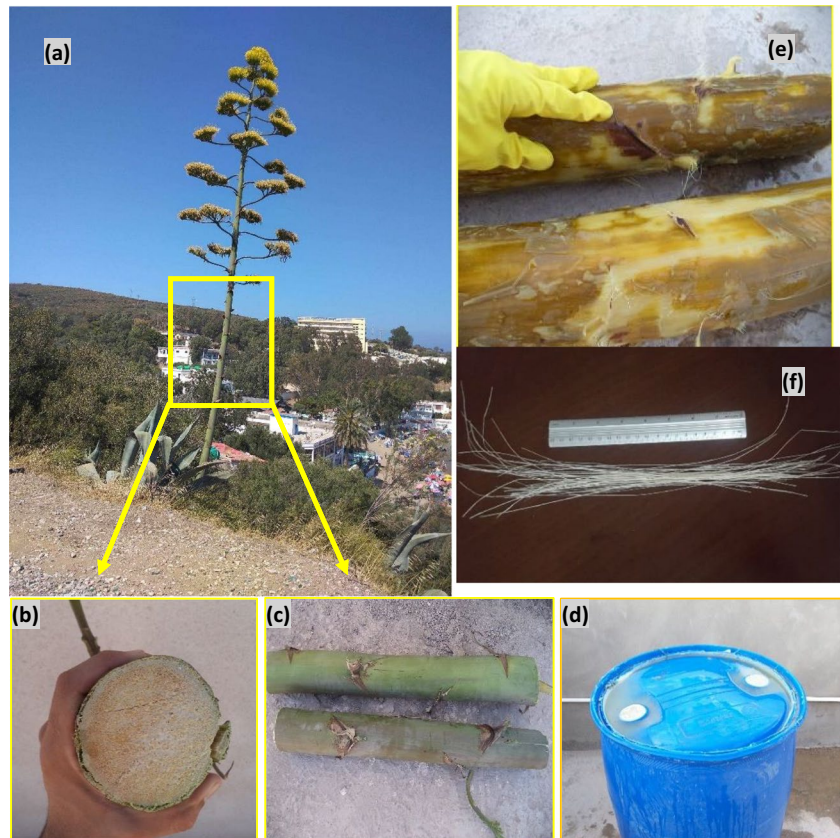
$$\rho_{FSAA} = \left[\frac{m_2 - m_1}{V_{py} - \frac{(m_3 - m_2)}{\rho_{acetone}}} \right] \quad (1)$$

2.2.2 Linear density

Each fiber's length was measured and then weighed using the single-fiber weighing method. It meets the requirements of ASTM D 2257, with the amount of removed fiber measured in Tex units. This method was widely used in the textile industry due to its reliability in determining fiber quality. The linear density was calculated using this data [31]. The following Eq. (2) to contrast the fiber's extracted fineness with that of other vegetable fibers:

$$Tex = \frac{weight(g)}{length(m)} \times 1000 \quad (2)$$

Fig. 1 **a** Flower stalk of *Agave americana* plant, **b–d** different steps for the immersion process of the FSAA, **e** biodegradation of fibers after 30 to 45 days at temperatures above 35 °C, **f** the FSAA fiber obtained



2.2.3 Moisture content and moisture regains

Working with natural fibers like cotton, wool, and flax requires careful consideration of several factors, including moisture content. These fibers had a propensity to take in moisture from the environment, which may have a substantial impact on their physical and mechanical characteristics. For this study, moisture content and moisture regains were determined according to test standard ASTM 2654 [32]. The usual weight-loss approach served as instrumental in determining the level of moisture and fiber recovery of FSAA fibers. Samples were weighed outside the oven before drying them at 100 ± 5 °C for 2 h.

To obtain a precise result, three samples were examined and calculated [31] using Eqs. (3) and (4).

$$\text{moistureregains}(\%) = \frac{\text{originalweight} - \text{ovendryweight}}{\text{Weightofdryfibersintheoven}} \times 100 \quad (3)$$

$$\text{Moisturecontent}(\%) = \frac{\text{originalweight} - \text{ovendryweight}}{\text{originalweight}} \times 100 \quad (4)$$

2.2.4 Fiber diameter

The width of each fiber was assessed employing an optical magnifier from ZEISS with a Plan-Achromat $\times 400$

lens. Three random locations over the length of the fiber were measured from each of the 30 samples and the single fiber's typical diameter was identified [31]. Based on these readings, a calculation was made to determine the typical diameter of the individual fibers with ZEN (Zeiss software). This methodology made sure that the fiber diameter was accurately and fairly analyzed for all samples.

2.2.5 Scanning electron microscopy (SEM) analysis

Micrographs were captured using a scanning electron microscope (SEM), the MEB-FEG Quattro S with a range of magnification settings and electron-accelerating voltages varying from 3 to 5 kV. To enhance electrical conductivity, improve image quality, protect the sample from potential damage, and reduce surface charging effects, the fiber had a gold covering applied to it. SEM is an effective imaging technique that can be used to analyze the microstructure of FSAA fibers and better understand their impact on mechanical characteristics. The resulting micrographs provided us with important new information about the morphological characteristics of the FSAA fibers, including their size, shape, and physical properties. Utilizing SEM allowed for a thorough analysis of the fibers at various magnifications, giving a thorough grasp of due to the morphology. Meb Quattro s in topographic mode was the instrument used to analyze fiber morphology.

2.2.6 Fourier transform infrared (FTIR) spectroscopic analysis

The existence of functional groups on the FSAA fibers was determined using an FTIR spectrometer, which recorded the IR spectra of the samples. PerkinElmer used infrared spectroscopy using a Fourier transform with a Spectrum RX1 to analyze the chemical features of the samples. The test was carried out by scanning 32 times over a spectral range of (4 cm^{-1}) , and in transmission mode 500 to 4000 cm^{-1} , according to the specified parameters. The Origin 10.0 software resolution application was used to carry out band deconvolution methods.

2.2.7 Thermogravimetric analysis (TGA) measurement

The ability of natural fibers to strengthen matrix polymers with high treatment temperatures depends on their ability to withstand thermal degradation. Traditional methods for instance, thermogravimetric (TG) and derived DTG, or thermogravimetric analysis, are often employed to assess the heat resistance of fibers. Analyses of TG and DTG are conducted to examine how the bulk and its amount of change vary as the temperature increases in FSAA fibers [33]. This study examined thermal stability using TGA/DSC 3 + 1600 °C (METTLER TOLEDO), for the fibers. An alumina beaker was placed in the oven with FSAA fibers inside. The test was conducted at an ambient temperature of 800 °C with a heating rate of 10 °C per minute. Another critical factor used to evaluate bio-fibers' thermal stability is their kinetic activation. The activation energy of motion is typically calculated using Brodido's formula (5) [21].

$$\ln \left[\ln \left(\frac{1}{y} \right) \right] = - \left(\frac{E_a}{R} \right) \left[\left(\frac{1}{T} \right) + K \right] \quad (5)$$

R is for the standard gas constant (8.32 J/mol K); T stands for Kelvin temperature; y is the standardized weight (w_t/w_i), and w_t and w_i stand for the sample's weight at different times and temperatures, respectively.

2.2.8 DSC (differential scanning calorimetry)

Differential scanning calorimetry was a common method to examine how materials react to heat. For natural fibers, DSC was employed to investigate their distinct thermal characteristics, including crystallinity, and transition of glass, temperature, melting point. Using this technique, the cellulose and lignin contents could be noted in the fibers' glass transition point temperature (T_g) and destruction temperature. The fibers were subjected manage cycles of heating and cooling to examine their thermal properties. METTLER TOLEDO

was the analysis using a thermogravimetry device used to capture the thermal events that took place when it is being heated, in the fiber.

2.2.9 X-ray diffraction (XRD) analysis

Using X-ray diffraction (XRD), the crystallinity index (CI) and crystallite size (CS) of FSAA fibers were calculated. When the FSAA fibers were exposed to X-rays, the crystals within the fibers scattered the X-rays, resulting in a distinct diffraction pattern that could be analyzed to determine the crystalline properties of the FSAA fiber. With a Bruker D8 ADVANCE Diffractometer for X-rays, radiation from a Cu-K source ($\lambda = 1.54184 \text{ \AA}$). The experiments were carried out at room temperature utilizing a generator using a 40 kV voltage and a 20 mA current. The samples, in powdered form, were examined within a specimen container by scanning them at 2 values between 10° and 70° with a $2^\circ/\text{min}$ progressive rate. The crystal size is determined by the following Eq. (6) [34]:

$$CS = \frac{K \cdot \lambda}{\beta \cdot \cos(\theta)} \quad (6)$$

The Scherrer constant is denoted by the sign K (0.9 (In Angstroms) represents the wavelength. β , which is the peak's overall breadth when it is half its greatest (in radians); and θ , which stands for the diffraction angle. Equation (7) is utilized to compute the crystallinity index [35]:

$$CI\% = \left[\frac{I_{002} - I_{am}}{I_{002}} \right] \times 100 \quad (7)$$

In Eq. 7, I_{002} stands for the crystalline region's greatest intensity, and I_{am} for the amorphous region's lowest intensity.

2.2.10 Water absorption

The study consists in tracking the samples changing cumulative mass after immersion in seawater and distilled water for 720 h (equivalent to 30 days) at an ambient temperature. The mass measurements were carried out at irregular intervals throughout a one-month duration following samples being submerged in seawater and distilled water. This approach was implemented to ensure a comprehensive assessment of the temporal changes in mass, thereby providing useful details about the effects of water immersion on the samples, without being restricted to predetermined time intervals for each measurement. Before weighing, the samples were carefully wiped with absorbent paper, and their mass was measured at regular intervals. An electronic scale of the OHAUS type was used for weighing (measurement

accuracy = 0.0001 g). The bulk gain associated with the aging of the fibers in the time % representation of t was used. The ASTM standard method D1037-99 was used to perform the water absorption tests [36]. The percentage change in weight of the FSAA fibers calculations was made at a specified time (t) using M_t (%), representing the weight change, expressed with the following equation:

$$M(t) = \frac{(m_t - m_0)}{m_0} \times 100 \quad (8)$$

According to a Peleg-proposed mathematical model, the fibers of FSAA's water adsorption curves were modified (Eq. 9).

$$g(t) = a + \frac{t}{b * t + c} \quad (9)$$

where the diffusion parameters, are stated in minutes, and a , b , and c are constants ($a=291.7$; $b=0.7457$; $c=0.2138$).

2.2.11 Tensile test of FSAA fibers

All experiments were performed at 25 °C with a relative humidity of about 62%. Tensile strength of a single fiber strength testing was performed using the Test112 global testing equipment after the fibers were glued to cardboard for stability. In 1 min, the crossbar moved 1 mm. Each sample was measured using a 100 mm GL (gauge length). Thirty different samples of FSAA fiber were analyzed to evaluate their elastic zone tensile properties. These properties included tensile strength, deformation, and young module. ASTM D3822-07, a method for measuring the tensile strength of textile fibers, was employed for the testing.

For natural fibers, statistical analysis plays a significant part in examining the fibers and composites. Through statistical analysis, mean values and variability of characteristics of FSAA fibers were determined. Fragile materials, where this technique had been previously applied multiple times, tended to fail due to the distribution of faults [37]. A two-parameter Weibull distribution was used to statistically assess the tensile mechanical characteristics of FSAA fibers, and the maximum likelihood technique (ML) was employed to estimate a 95% confidence interval for Young's modulus, fiber toughness, and strain. Minitab 19 [21] was employed to conduct the study's statistical analysis.

3 Results and discussion

3.1 Fiber density of FSAA fibers

An important instrument for assessing the strength, functionality, and condition of the fibers and tissues is the analysis of

fiber density. Natural fibers' density is impacted by a multitude of environmental and cultural factors, including plant age, fiber extraction method, soil quality, geographical area, and also plant space. Fiber density was 980 kg/m³ by using the overarching principle of the methodology (Eq. 1), the density of FSAA fibers is less than other fibers such as *Yucca treculeana* (1330 ± 39 kg/m³) [38], *Eleusine indica* (1143 kg/m³) [39], *Trachelospermum jasminoides* (1398 kg/m³) [40], *Acacia concinna* (1365 kg/m³) [41], *Typha augustata* grass (1015 kg/m³) [42], *Cocos nucifera* (1360 kg/m³) [43], *Cyperus dichrostachus* (1010 kg/m³) [44], *Fragrant screw pine* (13,852 kg/m³) [45], *Citrullus lanatus climber* (1227 ± 371 kg/m³) [46], *Ficus religiosa* root fibers (1246 kg/m³) [17], *Albizia amara* (1043 kg/m³) [47], and the FSAA fibers have a density greater than other fibers like vascular bundles stand of *Phoenix dactylifera* (914 kg/m³) [48], *Cyperus papyrus* plant (950 kg/m³) [31], *Furcraea selloa* k.koch Plant (810 kg/m³) [49], *Catalpa bignonioides* fruit (713 kg/m³) [14]. This may be due to the distinctive qualities of the flower stalk of *Agave americana* and the environmental circumstances in which it is grown. The physical characteristics of recently invented natural fibers are replicated in Table 1.

3.2 Linear density measurement

The FSAA fiber linear density is influenced by several factors, including the maturity of fiber included, growth circumstances, and extraction conditions. These elements contribute to defining how fine the fibers are overall, which in turn, affects the quality and potential applications of the material, the linear density calculation is an essential measure to assess the quality and properties of fibers. The linear density of the flower stalk of *Agave americana* fibers is determined in Tex units using Eq. (4). The typical fineness of the extracted fibers was 3.06 Tex. The linear density of FSAA fibers is superior to that of *Cyperus dichrostachus* fibers (0.51 ± 0.244 Tex) [44], and lower than that of *Cyperus papyrus* plant fibers (8.38 ± 0.6 Tex) [31].

3.3 Moisture regains and moisture content analysis

The moisture regain and moisture content of these fibers were estimated using Eqs. (2) and (3) at a temperature of (100 ± 5 °C) for 2 h, and the resulting value was 9.80%. The kiln dry weight method was employed for this calculation. There is 8.92% moisture in the material, FSSA fibers have a high moisture content than *Typha augustata* grass fibers (6.56%) [42], and lower than that of *Cyperus papyrus* (9.86%) [31]. The inherent hydrophilicity of natural fibers, which causes them to attract moisture from the environment, poses a challenge for composite reinforcement due to the impairs of the hydrophobic matrix and the fiber's interfacial adhesion [31].

Table 1 Comparison of the FSAA's physical characteristics with other cellulosic fibers

Name of the fiber	Density (kg/m ³)	Diameter (μm)	Reference
The flower stalk of <i>Agave americana</i>	980	208 ± 35	This work
Vascular bundles of <i>Phoenix dactylifera</i>	914	-	[48]
<i>Cocos nucifera</i>	1360	-	[43]
Fragrant screw pine	1385.2	280 ± 27	[45]
<i>Myriostachya wightiana</i>	1372–1510	102–278	[21]
<i>Albizia amara</i>	1043	-	[47]
<i>Yucca treculeana</i>	1330 ± 39	171 ± 36	[38]
<i>Eleusine indica</i>	1143	315.4 ± 10	[39]
<i>Trachospermum jasminoides</i>	1398	-	[40]
<i>Cyperus papyrus</i>	950	32.37 ± 0.81	[31]
<i>Furcraea selloa</i> k.koch	810	11.5	[49]
<i>Catalpa bignonioides</i> fruit	713	299	[14]
<i>Acacia concinna</i>	1365	-	[41]
<i>Typha angustata</i> grass	1015	105 ± 10.15	[42]
<i>Cyperus dichrostachus</i>	1010	9.85 ± 7.16	[44]
Areca palm leaf stalk	1090 ± 24	285–330	[50]
<i>Cyperus pangorei</i>	1102	133.3	[51]
<i>Catharanthus roseus</i>	1343	290.2	[52]
<i>Citrullus lanatus</i> climber	1227 ± 371	210 ± 4.85	[46]
<i>Ficus religiosa</i> root fiber	1246	25.62 ± 0.951	[17]

3.4 Diameter determination

The results of the analysis using an optical microscope to determine how large the fibers are, the microstructure and diameter distribution of the FSAA fiber are displayed in Fig. 2, and the fiber micrograph at 400× magnification in Fig. 2 reveals the fiber diameter. The fiber diameter was calculated to be three locations on the FSAA fiber, and it was found that the mean diameter was 208 ± 35 μm, this diameter measurement offers crucial details about the size and the fibers' morphology. The distribution of the observed fiber diameter is depicted as micrographs in Fig. 2, some other fibers have a diameter lower and higher than the FSAA fiber like *Citrullus lanatus* climber (210 ± 4.85 μm) [46], *Myriostachya wightiana* (102 ± 278 μm) [21], *Yucca treculeana* (171 ± 36 μm) [38], *Eleusine indica* (315.4 ± 10 μm) [39], and *Cyperus dichrostachus* (9.85 ± 7.16 μm) [44]. Table 1 displays the comparison with other fibers.

3.5 Scanning electron microscopy analysis (SEM) of FSAA fibers

The shape of the FSAA fiber's surface contained apparent imperfections, possibly due to wax or lignin, as determined by longitudinal and transverse examinations. Because of the roughness they add to the fiber's surface, these impurities can affect the material's or product's mechanical and physical properties. Increased friction between fibers is one effect of a fiber's rough surface, and contaminants can also

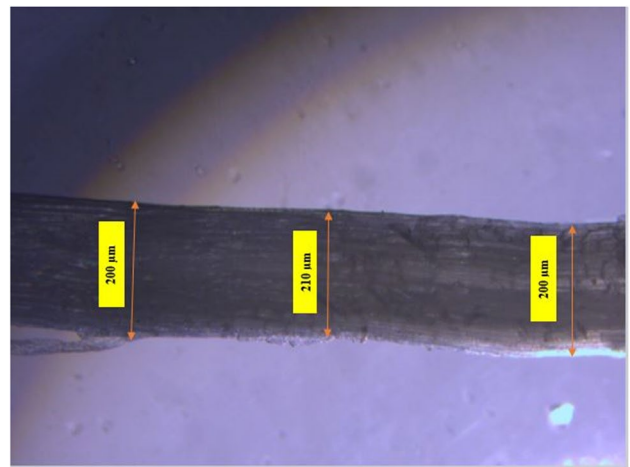


Fig. 2 Sample micrograph of an individual FSAA fiber

cause the fiber's surface to become rough and even hollow. Comparing the FSAA fiber with other fibers such as *Yucca treculeana* and fiber strands of *Phoenix dactylifera*, *Myriostachya wightiana* and fiber from *Juncus effusus*, it was found that they share similar surface characteristics and imperfections. This suggests that the presence of wax or lignin impurities, as well as the resulting roughness, may be common features among these fibers [21, 38, 48, 53]. Additionally, it was discovered that composite materials' mechanical toughness reinforced by natural fibers can be diminished because FSAA fibers had porosity along the surface of the

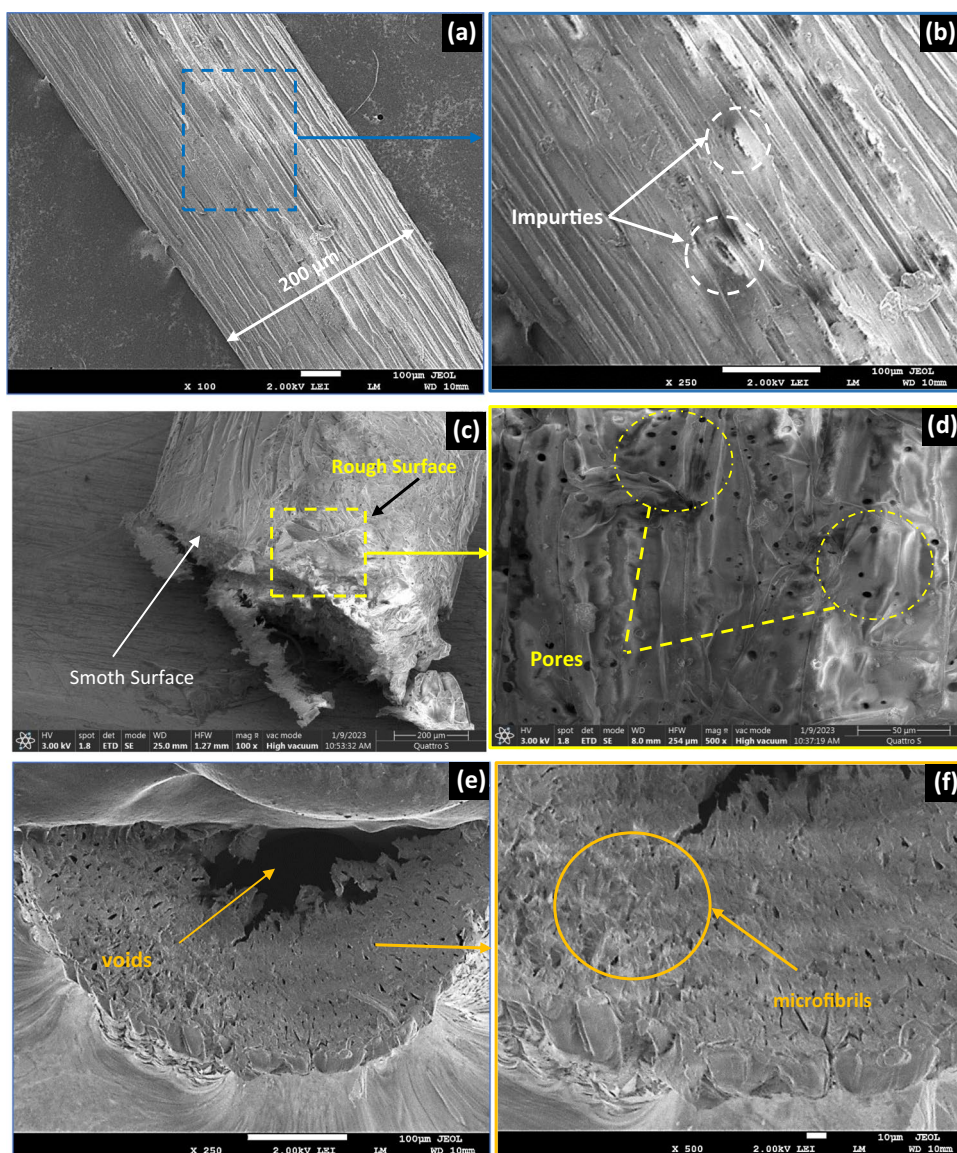
fiber that can make it more fragile and likely to break. The durability of a material is diminished because pores act as stress concentration areas and can lead to cracks or breaks. In addition to the width of the lines on the fibers' surface, the fiber arrangement displays alignment with the fiber axis's direction in the form of a consistently scattered square and semi-rectangular tray. The FSAA fiber exhibits a distinctive surface morphology characterized by irregularly distributed micropores or pits interspersed with microfibrils. Moreover, the surface shape of the fiber closely resembles an elliptical contour with an almost circular appearance [48]. This observation aligns with findings from previous investigations done on fibers originating from sources like *Catalpa bignonioides* fruits, *Washingtonia filifera*, and *Eleusine indica* grass [14, 39, 54]. These fibers also displayed similar features, including the presence of pores and microfibrils. The

fiber diameter that was measured is 200 μm . As observed in the fiber photograph Fig. 3a, the surface contains certain substances that could be contaminants, lignin, or wax as well as pores, the roughness of the fiber surface may be increased by these contaminants and imperfections [38], as shown in Fig. 3.

3.6 Fourier transform infrared (FTIR) spectroscopic analysis

The FTIR spectra for the FSAA fibers are shown in Fig. 4a. To analyze the FSAA fibers, the FTIR vibration spectrum was used to examine the absorption bands associated with functional chemical families, including cellulose, hemicelluloses, and lignin [55]. To resolve overlapping peaks

Fig. 3 SEM micrographs of the Longitudinal view of FSAA fiber with different magnifications



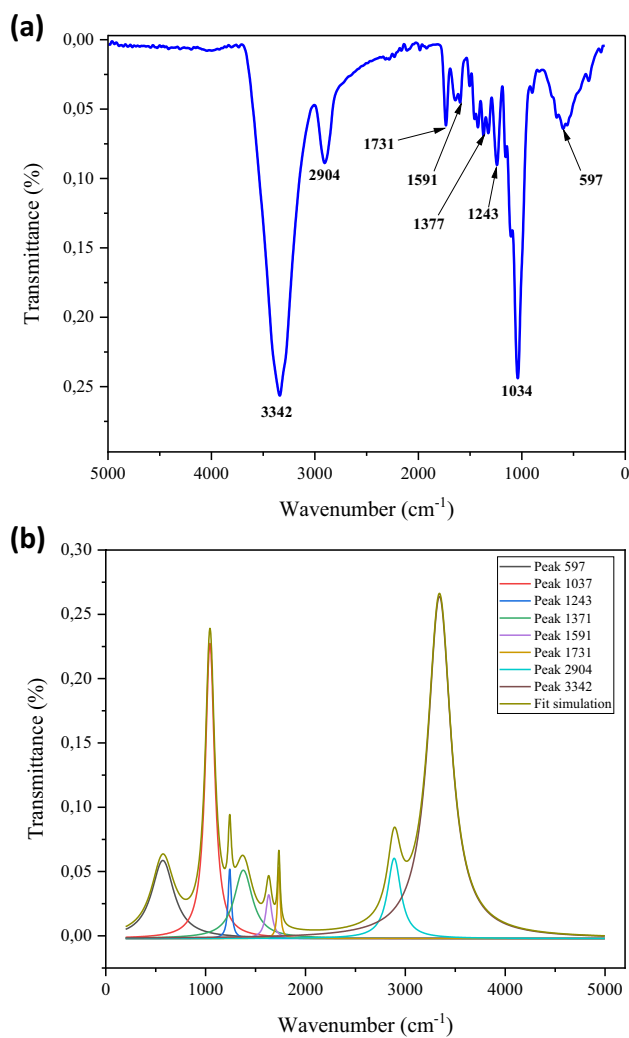


Fig. 4 FSAA FTIR analysis: **a** FTIR spectra and **b** deconvolution of peaks

in the complex spectra, peak deconvolution was applied specifically in the range of 500–4000 cm^{-1} (Fig. 4b). This technique allows for the separation and analysis of

individual peaks, providing a more detailed understanding of the molecular components and functional groups present in the FSAA fibers. The stretching vibrations of the hydroxyl groups (O–H) linked by hydrogen generated from cellulose cause the peak at 3342 cm^{-1} [21], whereas the maximum at 2904 cm^{-1} encoding cellulose and hemicelluloses are present, indicating the stretching vibration of the C–H from CH and CH_2 [56]. There are peaks in the frequency of FSAA fiber at 1731 cm^{-1} correlated to C=O stretching encoding the hemicellulose [15]. The aromatic ring of the phenyl propane molecule C=C in lignin is what causes the peak at 1591 cm^{-1} [52]. The peaks from the spectrum analysis were compared to those from other works, which are listed in Table 2. C–H Bending vibration is responsible for the highest point seen at 1377 cm^{-1} [57]. We notice a peak at 1243 cm^{-1} caused by the C–O extending the vibration of the acetyl group in lignin [38]. The FTIR spectrum showed dual peaks at 1034 cm^{-1} which are about C–O and O–H indicating the occurrence of lignin. On the other hand, the C–OH bending generates an absorbance peak of around 597 cm^{-1} [58], and it can be inferred that the CO–H group out-of-plane bending exists.

3.7 Thermogravimetric analysis (TGA) measurement

The thermogravimetric analysis (TGA) and its derivative (DTG) are graphically depicted in Fig. 5a. Two separate mass loss phases can be seen in the TGA curves. During the first phase of mass loss, 9% between room temperature and $100 \text{ }^\circ\text{C}$ is determined by a DTG peak plot at $75.27 \text{ }^\circ\text{C}$ inferred from the fiber's dehydration [55]. The following stage of mass loss was 56.52% between 200 and $359 \text{ }^\circ\text{C}$, meaning hemicellulose and cellulose combined mass loss. The DTG curves display clear peaks at degradation temperature of $339.57 \text{ }^\circ\text{C}$, which was found to be the point where fibers begin to fall apart. Figure 5b's $\ln [\ln (1/y)]$ plot vs. $1/T$, this straight line

Table 2 Observation of FTIR peaks for FSAA fiber

Peak position in this study (cm^{-1})	Range of peak reference values (cm^{-1})	Functional group and chemical composition	Reference
3342	3449–2912.33	Hydrogen-bonded O–H stretching in α cellulose	[21]
2904	2909–2851	the presence of cellulose and hemicelluloses, represents the C–H stretching vibration from CH and CH_2	[56]
1731	1731–1636	C=O stretching encodes the hemicellulose	[15]
1591	1591–1629	the aromatic ring of the phenyl propane molecule C=C in lignin	[52]
1377	1379–2936	C–H Bending vibration	[57]
1243	1242	C–O stretching vibration of the acetyl group in lignin	[38]
1034	1035	C–O and O–H indicating the occurrence of lignin	[58]
597	598	C–OH bending	[58]

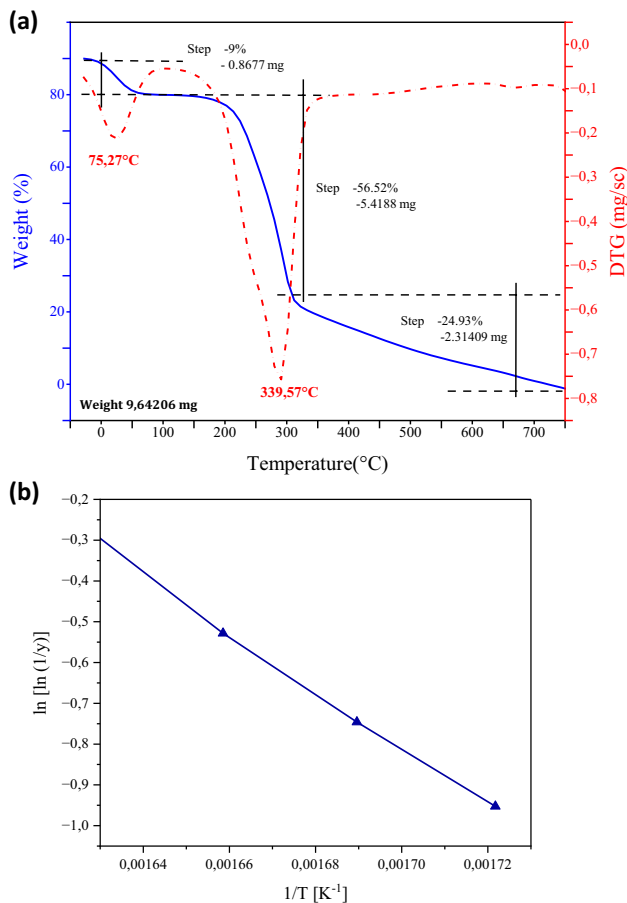


Fig. 5 **a** TG and DTG curves of the thermal analysis of the FSAA fiber, **b** Broido's plot

obtained from the data, is employed to determine the activation energy (E_a) using Eq. (5), which was discovered to be 68.1 kJ/mol. This is superior to the fiber of

the *Leucaena leucocephala* tree (64.22 kJ/mol) [33], and *Typha angustata* grass (67.99 kJ/mol) [42], (64.38 kJ/mol) for *Phaseolus vulgaris* [20], and less compared to the *Banyan* tree's aerial roots fiber (72.65 kJ/mol) [59], and *Myriostachya wightiana* (72.84 kJ/mol) [21], *Fragrant screw pine* (83.9 kJ/mol) [45], *Acacia nilotica* (69.739 kJ/mol) [60]. Table 3 shows the FSAA fiber's thermal characteristics and the kinetics activation energy in comparison with other cellulosic fibers.

3.8 DSC (differential scanning calorimetry)

DSC analysis enables the identification of thermal transitions by examining physical changes caused by the absorption and release of thermal energy during heating. Figure 6 shows the DSC analysis of the fibers of FSAA. The initial temperature peak, indicating an endothermic process, was measured at 76 °C and was caused by the moisture evaporating from the fibers. The peak's associated integrated enthalpy was 2015.61 mJ. The second peak, which was reached at 274 °C, revealed that polysaccharides other than lignin, namely α -cellulose, were decomposing. The next endothermic peak is 318 °C in a nitrogen atmosphere, the peak represents α -cellulose degradation in the FSAA fibers [65]. The surface's cellulose content had completely degraded, as evidenced by the subsequent significant endothermic peak at 362 °C [66].

3.9 X-ray diffraction analysis (XRD)

Three peaks were observed after the profiles of X-ray diffraction were deconvoluted (Fig. 7). The cellulose's crystalline phase is shown by the other peaks at 21.67° (002) and 30.12° (004); however, the first peak at 15.57° (110)

Table 3 Thermal characteristics comparison between the FSAA and other cellulosic fibers

Fiber	Energy for kinetic activation (kJ/mol)	Maximum degradation temperature (°C)	Reference
Flower stalk of <i>Agave americana</i>	68.15	339.57	This work
<i>Leucaena leucocephala</i>	64.22	312.64	[33]
<i>Ficus religiosa</i> root fiber	68.02	400	[17]
<i>Cissus vitiginea</i>	68.72	304	[61]
<i>Typha angustata</i> grass	67.99	-	[42]
<i>Myriostachya wightiana</i>	72.84	-	[21]
<i>Acacia nilotica</i>	69.739	-	[60]
<i>Lygeum spartum</i>	68.77	338.7	[62]
Red banana peduncle	-	353	[63]
<i>Fragrant screw pine</i>	83.9	321.4	[45]
Aerial roots of <i>banyan</i> tree	72.65	358	[59]
<i>Dracaena reflexa</i>	68.784	348.78	[64]
<i>Phaseolus vulgaris</i>	64.38	328.5	[20]

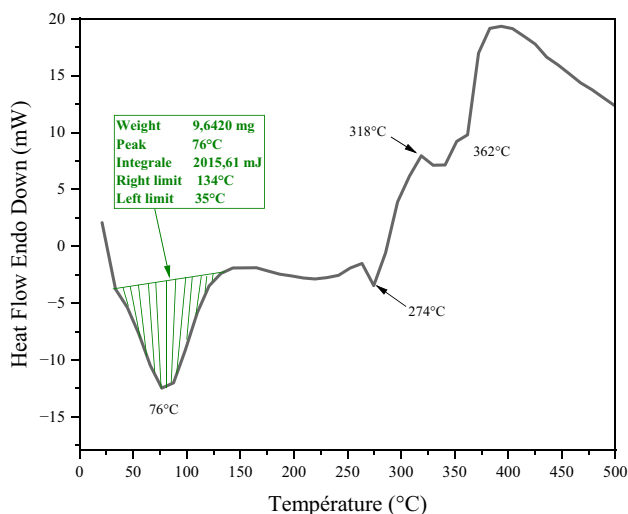


Fig. 6 DSC curves of FSAA fiber

indicates the fiber’s amorphous phase. Using Eq. (7), the crystallinity index (CI) was estimated to be 29.15%, far smaller compared to that of *Zingiber officinale* (78.81%) [67], *Cocos nucifera* (52%) [43], and *Catalpa bignonioides* fruit (94%) [14], but larger than that of *Acacia concinna* (27.5%) [41]. Using Scherrer’s Eq. (6) to compute the crystalline size, the result was (2.53 nm), which is lower than other fibers such as *Tithonia diversifolia* (3 nm) [55], *Yucca treculeana* (3.02 nm) [38], *Cocos nucifera* (6.5 nm) [43], and higher than that of *Leucaena leucocephala* (2.33 nm) [33]. A comparison with the referenced publications is provided in Table 4. FSAA fibers have been

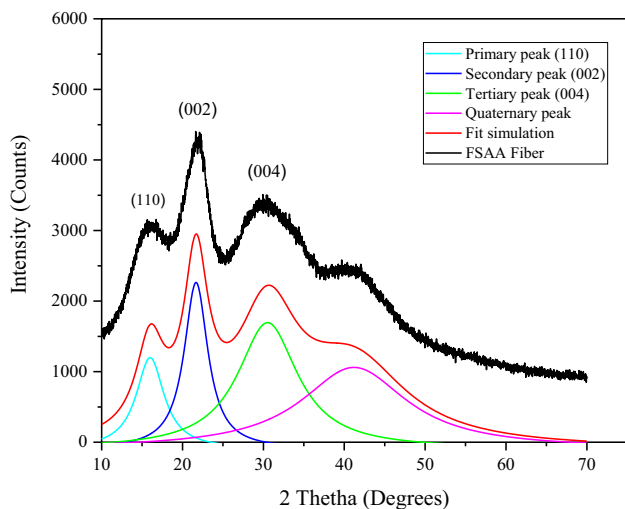


Fig. 7 XRD spectrum of FSAA fiber

found to have crystalline properties. The fiber’s properties are sufficiently strong to enable its utilization as reinforcement in composites.

3.10 Water absorption

From Fig. 8, it appears that natural fibers have a significant capacity to absorb water, regardless of whether they are submerged in distilled water or seawater. After 24 h of submersion (1440 min), it shows that they can adsorb as much as 850% and 868% of their relative dry weights for distilled and sea water which exceeds that of *Washingtonia filifera* fibers (220% of their initial mass) [54]. The fibers possess a high absorption capacity due to the presence of cellulose and its porous structure [54]. It is crucial to remember that the absorption of water by natural fibers can have consequences on their properties, such as their strength, elasticity, and softness. This must be considered when they are used for the production of textiles and other products [70]. After 360 and 720 h of water immersion, the value of absorption did not change. It is possible to say that the mathematical formula which allows the explanation for the kinetics of the body absorbing water in the FSSA fibers is given by the mathematical model found in the literature and was used to study the distilled water absorption and seawater absorption kinetics in the FSAA fibers. Better statistical parameters for sampling areas can be found in the pelagic model [71]. We can see from Fig. 8a and b that the proposed model maximizes the number of experimental points such closely as is physically possible [72].

Table 4 The comparison of the crystallographic qualities of FSAA fiber with other cellulosic fibers

Fiber	Crystalline properties		Reference
	Ci (%)	Cs (nm)	
Flower stalk of <i>Agave americana</i>	29.15	2.53	This work
<i>Yucca treculeana</i>	48.85	3.02	[38]
<i>Eleusine indica</i>	45	-	[39]
<i>Leucaena leucocephala</i>	63.10	2.33	[33]
<i>Trachelospermum jasminoides</i>	87.68	3.9	[40]
<i>Cocos nucifera</i>	53	6.5	[43]
<i>Ageratina adenophora</i>	68.98	16.28 ± 1.55	[68]
<i>Catalpa bignonioides</i> fruit	94	-	[14]
<i>Typha augustata</i> grass	65.16	6.40	[42]
<i>Albizia amara</i>	63.7	-	[47]
<i>Citrullus lanatus</i> climber	35.70	16.30	[46]
<i>Acacia nilotica</i>	44.82	3.21	[60]
<i>Acacia concinna</i>	27.5	4.17	[41]
<i>Zingiber officinale</i>	78.81	-	[67]
<i>Tithonia diversifolia</i>	45	3.00	[55]
<i>Yucca gloriosa</i>	37.74	-	[69]
<i>Myriostachya wightiana</i>	54.799	3.24	[21]

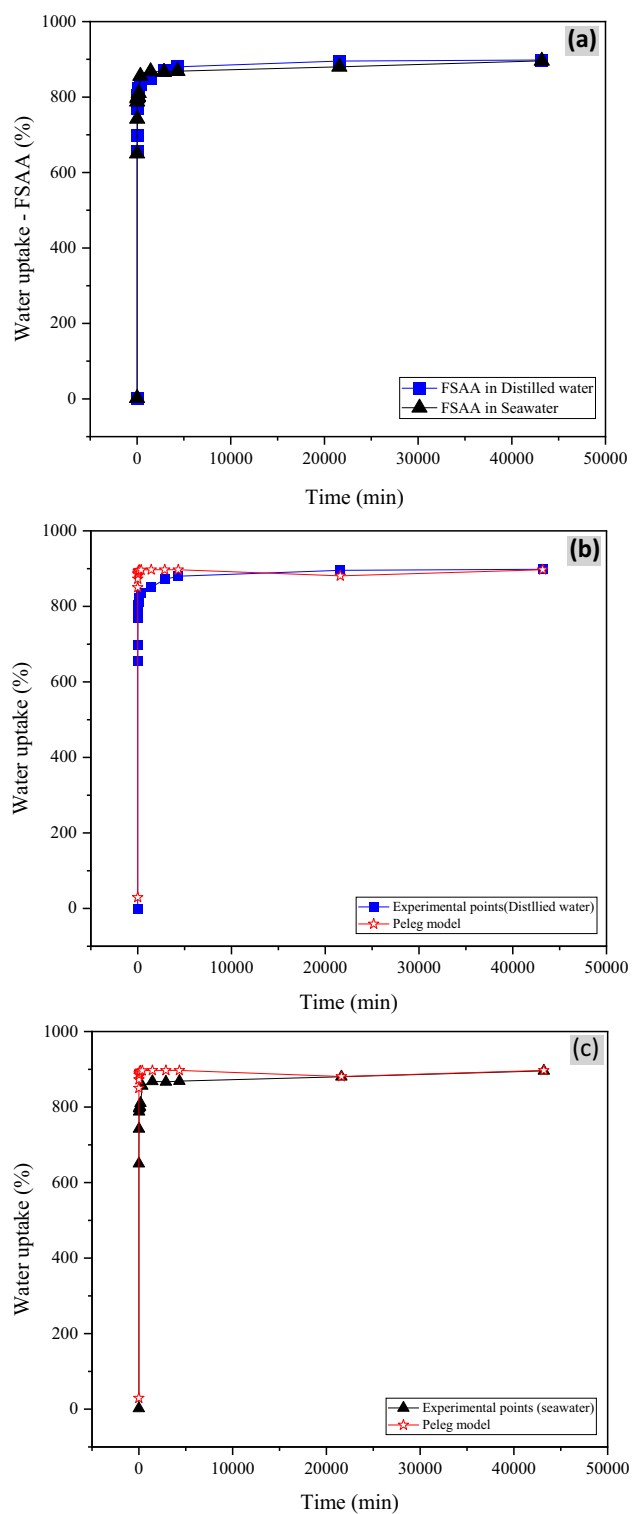


Fig. 8 FSAA water absorption curves: **a** FSAA water absorption behavior, **b** Peleg modeling for distilled water, and **c** Peleg modeling for seawater water

3.11 Tensile test of FSAA fibers

Quasi-static tensile testing of the FSAA fibers was completed at a constant 1 mm per minute speed and a length of 100 mm. A collection of 30 carefully selected specimens composed of these fibers was created. Figure 9a illustrates the standard stress–strain curve of individual FSAA fibers. The FSAA fiber exhibits exceptionally brittle behavior and a rapid low-load failure in the case of a fiber failure. Tensile assessment of a single FSAA fiber shows a two-phase response to stress and strain (Fig. 9a), exhibiting brittle behavior similar to that of the *Yucca treuculana* [38]. The following phase was reached when the fiber ruptured or when the strain suddenly decreased to an average value of $(64.34 \pm 11.43 \text{ MPa})$. The fiber's tensile strength surpassed that of regularly used fibers, including *Myriostachya wightiana* 46.554 MPa [21], and lower than that of *Ageratina* phase was characterized by a linear zone with a strain ranging from 0 to 1.57%. Young's modulus for strain levels ranging from 0 to 0.8% was calculated using the elastic zone with a very steep slope of the curve $(77.61 \pm 15.90 \text{ GPa})$ (Fig. 9a). The FSAA fibers had a significantly higher Young's modulus than other types of fibers than that of the *Juncus effusus* $(4.38 \pm 1.37 \text{ GPa})$ [53], and *Yucca treculeana* $(16.85 \pm 10.52 \text{ GPa})$ [38]. Table 5 presents an overview of the mechanical characteristics of the tested fibers and contrasts them with FSAA fibers. Furthermore, it should be noted that for some experiments in the second phase, the fiber occasionally exhibited discontinuities that were mostly caused by the rupture of some microfibrillar structures. The same behavior for different GL between 10 and 40 mm was observed for *Agave americana* fibers [57]. Young's modulus, strain at failure, and strength under tension are displayed in Fig. 9b, c, and d, respectively. As is typical of lignocellulosic fibers, the data demonstrate a significant degree of dispersion, and the conclusions must therefore be properly understood through statistical examination of the data. Furthermore, other factors that affect experimental testing include test settings and characteristics such as test speed, machine accuracy, machine grip style, and measurement of fiber cross-sections to gauge strength [54].

The FSAA fiber exhibits exceptionally brittle behavior and a rapid low-load failure in the case of a fiber failure. Figure 10a–c displays the Weibull distribution plot curves for the FSAA fibers' Young's modulus, tensile strength, and strain at failure. Each fiber's values for tensile strength, strain at failure, and Young's modulus were determined to fall within the range and to perfectly fit the Weibull distribution. The Weibull graphs' scale factors and shape

Fig. 9 Property tensile of FSAA fibers **a** stress/strained behavior, **b** diameter versus tensile strength, **c** failure strain versus fiber diameter, and **d** Young’s modulus versus fiber diameter for GL = 100 mm

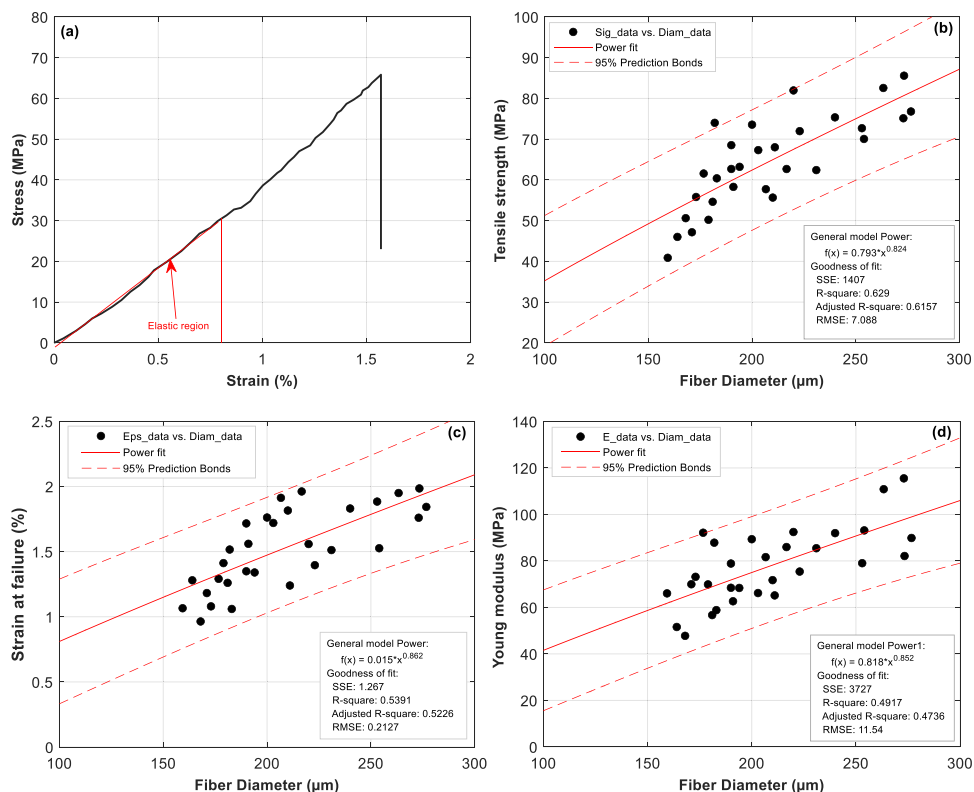


Table 5 Mechanical properties comparison of FSAA fiber with those from other plants reported in published publications

Fiber	GL (mm)	Tensile strength (MPa)	Young’s modulus (GPa)	Elongation at break (%)	Reference
Flower stalk of <i>Agave americana</i>	100	64.34 ± 11.43	77.61 ± 15.90	1.52 ± 0.31	This work
<i>Yucca treculeana</i>	40	222.13 ± 124	16.85 ± 10.52	2.75 ± 0.6	[38]
<i>Juncus effusus</i>	40	113 ± 36	4.38 ± 1.37	4.36	[53]
<i>Fragrant screw pine</i>	50	915 ± 195	33 ± 9	4.59 ± 2.17	[45]
<i>Ageratina adenophora</i>	50	123 ± 9.04	7.69 ± 0.94	1.6 ± 0.47	[68]
<i>Albizia amara</i>	50	640 ± 13.4	-	1.57 ± 0.04	[47]
<i>Myriostachya wightiana</i>	20	46.554	2.442	3.60 ± 0.95	[21]
Fiber strands of <i>Phoenix dactylifera</i>	30	530.5 ± 115.2	21.90 ± 3.96	2.47 ± 1.04	[48]

were employed to verify the findings of the experiments. The homogeneity of the distribution of the experimental data is confirmed by the shape factor utilized in this study [37], ($m_E = 5.2$ for Young’s modulus, $m_\sigma = 6.5$ for strain at failure, and $m_\epsilon = 5.8$). The scale factor values that were anticipated for the present study were 69.14 MPa, 1.64%, and 84.04 GPa. Where, respectively, represent the tensile strength, strain at failure, and Young’s modulus. These numbers perfectly match the average observed trial results at 64.34 ± 11.43 MPa, $1.5 \pm 0.31\%$, and 77.61 ± 15.90 GPa. Figure 11a–c plots illustrate the probability of survival (P) for the 2-parameter Weibull using FSAA fibers’

mechanical characteristics. The study’s findings demonstrate that the ML approach combined with the two-parameter Weibull distribution yields mechanical properties that exhibit comparability to the median observed findings of the experiment. Young’s modulus, strain at failure, and tensile strength are each depicted in Fig. 11a, b, and c, respectively. Lower mechanical property values have a high probability of survival. Tensile strength, strain, and tensile modulus values for the FSAA fibers for GL = 100 of 54.13 MPa, 1.24%, and 63 GPa, respectively, are needed to ensure 50% FSAA fibers survival, corresponding to a probability of $P(\sigma) = P(\epsilon) = P(E) = 0.5$.

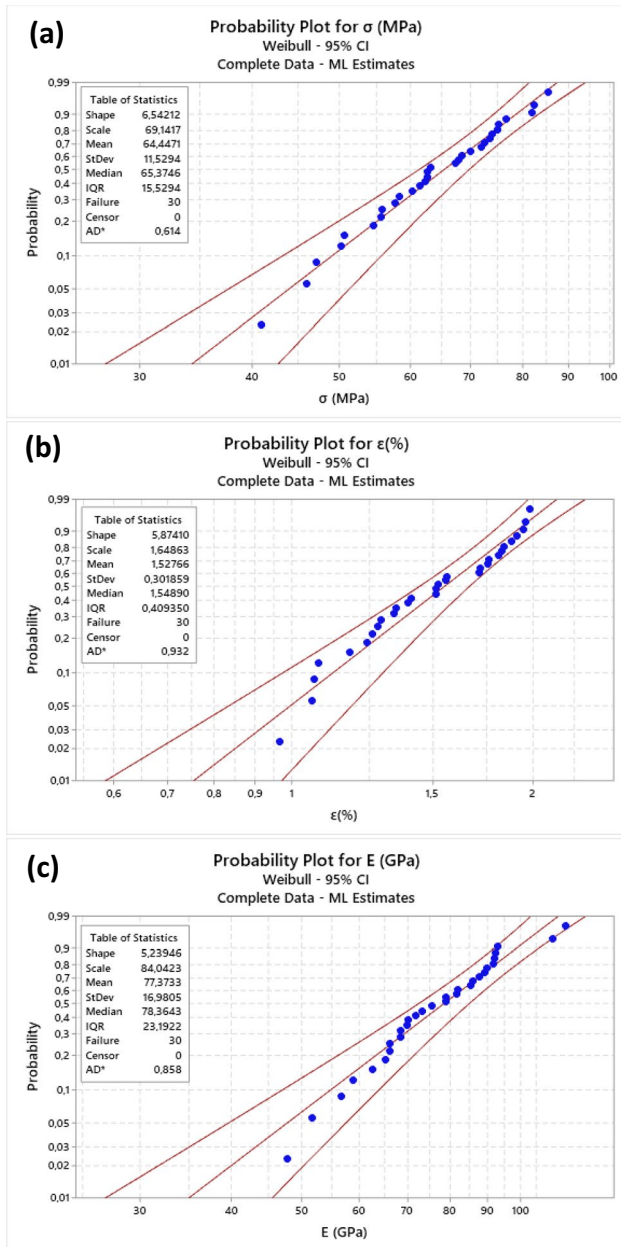


Fig. 10 Weibull distribution with two parameters for mechanical properties of the FSAA for ML method. **a** Tensile strength, **b** elongation at break, and **c** Young's modulus

4 Conclusions

In conclusion, our research aimed to investigate and comprehend the properties of fiber obtained from the *Agave* plant's flower stalk, with a particular focus on its viability as a reinforcing component in biocomposite materials. According to our findings, these fibers have promising qualities that point to their potential for use in these kinds of applications. As a result, this research moves us one step closer to a day when ecologically friendly options are essential in the materials

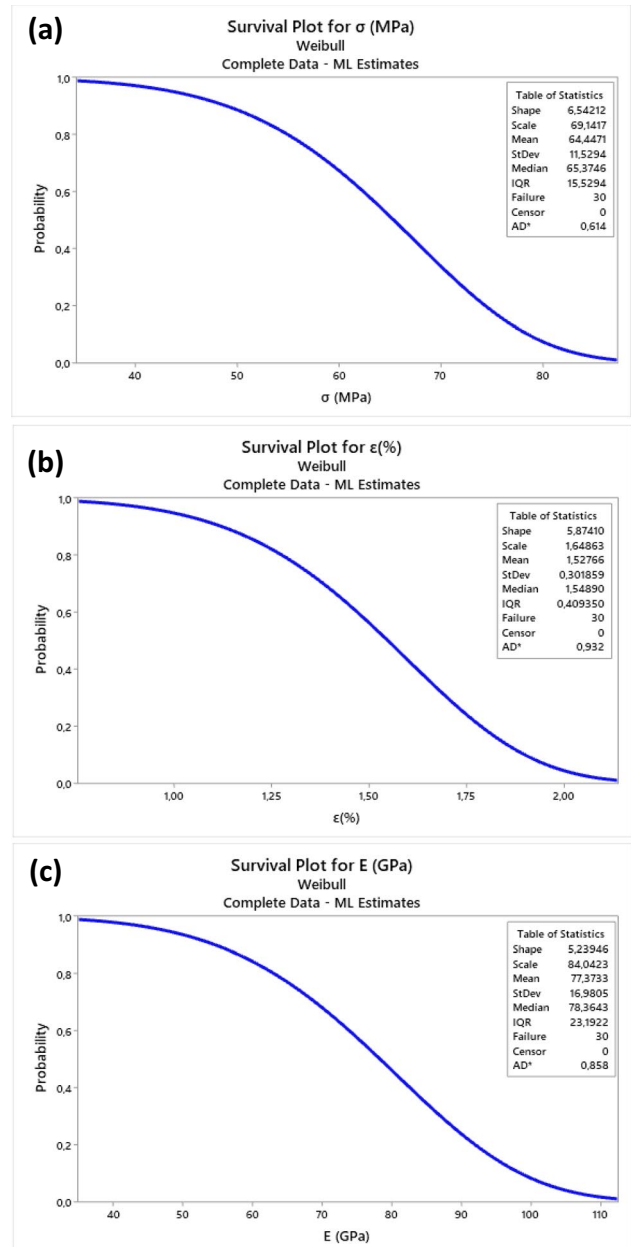


Fig. 11 Probability of survival graphs of mechanical properties of FSAA with 2-parameter Weibull for ML method

business. The morphological, mechanical, chemical, thermal, and physical characteristics of FSAA fibers, which have a density of 980 kg/m^3 , were examined in this study.

The average diameter of the FSAA was approximately ($208 \pm 35 \mu\text{m}$).

- FSAA fibers are well suited for low humidity applications due to their elevated moisture recapture (9.80%) and content (8.92%). However, the strength of the interfacial adhesion in reinforced composites may be impacted by their hydrophilic character.

- The existence of wax (C–C), lignin (C=C), hemicellulose (O–H), and cellulose (O=C) was confirmed using FTIR analysis.
- The XRD analysis confirmed that the CI of FSAA is 29.15%, the CS is 2.53 nm.
- The kinetic activation energy of the fibers was determined to be 68.15 kJ/mol using Broido's figure. The degradation temperature of 339.57 °C has been identified as the threshold at which the fibers begin to disintegrate. The thermal stability of the fibers is maintained between 200 and 250 °C. Beyond this range, the fibers start to deteriorate, leading to changes in their mechanical and physical properties.
- It appears that the fibers can absorb eight times the dry weight in the first 72 h, reaching 880% and 868% for distilled water and seawater, respectively. The Peleg model was used to simulate the kinetics of distilled water and seawater absorption and provided improved statistical parameters when used with experimental data.
- The mechanical characteristics of thirty sample fibers (FSAA) tested in quasi-static tension showed a high Young's modulus (77.61 ± 15.90 GPa) and with an average ultimate tensile stress of ($\sigma = 64.34 \pm 11.43$ MPa), strain at failure of ($1.5 \pm 0.31\%$).
- The two specifications for the FSAA fibers, the Weibull modulus was calculated using the ML technique using the strength (m_σ), and Young's modulus (m_E), strain at break (m_ϵ).

The experimental research in this work supported and confirmed the usage of fibers from the flower stalk of the *Agave americana* as reinforcement in novel composite materials used to produce biodegradable and biocompatible such as materials for medical implants, dressings, and drug delivery systems, and reinforced the materials, bumpers, dashboards, and door panels.

Author contribution Imen Lalaymia: this work involved the following processes — conceptualization, inquiry, methodology, writing, review, and editing. Ahmed Belaadi: conceptualization, investigation, methodology, supervision, writing, and review/editing were all integral parts of this work. Azzeddine Bedjaoui: methodology, investigation, and writing, including review and editing, were carried out for this work. Hassan Alshahrani: investigation and writing — review and editing. Mohammad K. A. Khan: investigation and writing — review and editing.

Funding The authors express their gratitude to the Deanship of Scientific Research at Najran University for providing funding for this work through the Research Groups Funding program grant code (NU/RG/SERC/12/24).

Data availability Not applicable.

Code availability Not applicable.

Declarations

Ethics approval The work adheres to ethical standards, containing no libelous or unlawful statements. It respects the rights of others and does not include any material or instructions that may cause harm or injury.

Consent to participate The authors consent to participate.

Consent for publication The authors consent to publish.

Competing interests The authors declare no competing interests.

References

1. Rajeshkumar G, Devnani GL, Maran JP et al (2021) Characterization of novel natural cellulosic fibers from purple bauhinia for potential reinforcement in polymer composites. *Cellulose* 28:5373–5385. <https://doi.org/10.1007/s10570-021-03919-2>
2. Sanjay MR, Siengchin S, Parameswaranpillai J et al (2019) A comprehensive review of techniques for natural fibers as reinforcement in composites : preparation, processing and characterization. *Carbohydr Polym* 207:108–121. <https://doi.org/10.1016/j.carbpol.2018.11.083>
3. Sanjay MR, Madhu P, Jawaid M, Sentharamaikannan P, Senthil S, Pradeep S (2018) Characterization and properties of natural fiber polymer composites: a comprehensive review. *J Clean Prod* 172:566–581. <https://doi.org/10.1016/j.jclepro.2017.10.101>
4. Rice MP, Meurah T, Mahlia I et al (2019) Mechanical and thermal properties of montmorillonite-reinforced polypropylene/rice husk hybrid nanocomposites. *Polymers (Basel)* 11. <https://doi.org/10.3390/polym11101557>
5. Indran S, Raj RE (2015) Characterization of new natural cellulosic fiber from *Cissus quadrangularis* stem. *Carbohydr Polym* 117:392–399. <https://doi.org/10.1016/j.carbpol.2014.09.072>
6. Pappu A, Pickering KL, Kumar V (2019) Manufacturing and characterization of sustainable hybrid composites using sisal and hemp fibres as reinforcement of poly (lactic acid) via injection moulding. *Ind Crop Prod* 137:260–269. <https://doi.org/10.1016/j.indcrop.2019.05.040>
7. Sultana N, Hossain SMZ, Alam S et al (2020) An experimental investigation and modeling approach of response surface methodology coupled with crow search algorithm for optimizing the properties of jute fiber reinforced concrete. *Constr Build Mater* 243:118216. <https://doi.org/10.1016/j.conbuildmat.2020.118216>
8. Ramasamy M, Arul A, Nithya M et al (2021) Characterization of natural – synthetic fiber reinforced epoxy based composite – hybridization of kenaf fiber and kevlar fiber. *Mater Today Proc* 37:1699–1705. <https://doi.org/10.1016/j.matpr.2020.07.243>
9. Badanayak P, Jose S, Bose G (2023) Banana pseudostem fiber : a critical review on fiber extraction , characterization , and surface modification. *J Nat Fibers* 20. <https://doi.org/10.1080/15440478.2023.2168821>
10. Sharma RP, Dixit J, Jaiswal A, Sharma N (2018) Mechanical testing of new natural fibre reinforced composite material. *Int J Tech Res Sci Spec* 29–39. <https://doi.org/10.30780/specialissue-icrdet-2021/007>
11. Madhu P, Sanjay MR, Sentharamaikannan P et al (2019) A review on synthesis and characterization of commercially available natural fibers: Part-I. *J Nat Fibers* 16:1132–1144. <https://doi.org/10.1080/15440478.2018.1453433>
12. Du H, Liu W, Zhang M et al (2019) Cellulose nanocrystals and cellulose nano fibrils based hydrogels for biomedical applications.

- Carbohydr Polym 209:130–144. <https://doi.org/10.1016/j.carbpol.2019.01.020>
13. Satha H, Kouadri I, Benachour D (2020) Thermal, structural and morphological studies of cellulose and cellulose nanofibers extracted from bitter watermelon of the Cucurbitaceae family. *J Polym Environ* 28:1914–1920. <https://doi.org/10.1007/s10924-020-01735-6>
 14. Bozaci E, Tağaç AA (2022) Extraction and characterization of new cellulosic fiber from catalpa bignonioides fruits for potential use in sustainable products. *Polymers (Basel)* 15. <https://doi.org/10.3390/polym15010201>
 15. Feleke K, Thothadri G, Beri Tufa H et al (2023) Extraction and characterization of fiber and cellulose from Ethiopian linseed straw: determination of retting period and optimization of multi-step alkaline peroxide process. *Polymers (Basel)* 15. <https://doi.org/10.3390/polym15020469>
 16. Nagarajaganesh B, Ganeshan P, Ramshankar P, Raja K (2019) Assessment of natural cellulosic fibers derived from Senna auriculata for making light weight industrial biocomposites. *Ind Crop Prod* 139. <https://doi.org/10.1016/j.indcrop.2019.111546>
 17. Marcel AA, Ravindran D, Bharathi SRS et al (2020) Characterization of a new cellulosic natural fiber extracted from the root of Ficus religiosa tree. *Int J Biol Macromol* 142:212–221. <https://doi.org/10.1016/j.ijbiomac.2019.09.094>
 18. Kathirselvam M, Kumaravel A, Arthanarieswaran VP, Saravankumar SS (2019) Assessment of cellulose in bark fibers of Thespesia populnea : influence of stem maturity on fiber characterization. *Carbohydr Polym* 212:439–449. <https://doi.org/10.1016/j.carbpol.2019.02.072>
 19. Cheng D, Weng B, Chen Y et al (2020) Characterization of potential cellulose fiber from Luffa vine : a study on physicochemical and structural properties. *Int J Biol Macromol* 164:2247–2257. <https://doi.org/10.1016/j.ijbiomac.2020.08.098>
 20. Babu BG, Princewinston D, Senthamaraiannan P et al (2018) Study on characterization and physicochemical properties of new natural fiber from Phaseolus vulgaris. *J Nat Fibers* 16:1035–1042. <https://doi.org/10.1080/15440478.2018.1448318>
 21. Parida PK, Pradhan AK, Pandit MK (2023) Characterization of cellulose fiber extracted from stems of Myriostachya wightiana (MW) plants: a viable reinforcement for polymer composite. *Fibers Polym* 24:489–503. <https://doi.org/10.1007/s12221-023-00020-2>
 22. Maran M, Kumar R, Senthamaraiannan P (2020) Suitability evaluation of Sida mysorensis plant fiber as reinforcement in polymer composite. *J Nat Fibers* 19:1659–1669. <https://doi.org/10.1080/15440478.2020.1787920>
 23. Mansouri A, Ben Nasr J, Ben Amar M, Elhalouani F (2020) Characterization of fiber extracted from Agave americana after burial in soil. *Fibers Polym* 21:724–732. <https://doi.org/10.1007/s12221-020-8666-9>
 24. Gerald Arul Selvan MT, Binoj JS, Mansingh BB, Baby Sajin JA (2023) Physico-chemical properties of alkali treated cellulosic fibers from fragrant screw pine prop root. *J Nat Fibers* 20:148–161. <https://doi.org/10.1080/15440478.2022.2129897>
 25. Saraswat BK, Sharma VK, Sharma R (2023) Alkali treatment effects on agave Americana fiber properties. *Mater Today Proc.* <https://doi.org/10.1016/j.matpr.2023.03.035>
 26. Ali M, Alabdulkarem A, Nuhait A et al (2020) Thermal analyses of loose Agave, wheat straw fibers and Agave / wheat straw as new hybrid thermal insulating materials for buildings. *J Nat Fibers* 18:2173–2188. <https://doi.org/10.1080/15440478.2020.1724232>
 27. Mancino A, Marannano G, Zuccarello B, Mancino A (2018) Implementation of eco-sustainable biocomposite materials reinforced by optimized agave fibers. *Procedia Struct Integr* 8:526–538. <https://doi.org/10.1016/j.prostr.2017.12.052>
 28. Sathiamurthi P, Karthi Vinith KS, Sathishkumar TP, Arunkumar S, Anaamalaai AS (2021) Fiber extraction and mechanical properties of Agave Americana/Kenaf fiber reinforced hybrid epoxy composite. *Mater Today: Proc* 46(Part 17):8594–8601. <https://doi.org/10.1016/j.matpr.2021.03.571>
 29. Torres-Tello EV, Robledo-Ortíz JR, González-García Y et al (2017) Effect of agave fiber content in the thermal and mechanical properties of green composites based on polyhydroxybutyrate or poly(hydroxybutyrate-co-hydroxyvalerate). *Ind Crops Prod* 99:117–125. <https://doi.org/10.1016/j.indcrop.2017.01.035>
 30. Mehrez I, Hachem H, Gheith R et al (2022) Optimization of mortar / Agave americana fibers composite behavior based on experimental design. *J Nat Fibers* 20. <https://doi.org/10.1080/15440478.2022.2152149>
 31. Sheferaw L, Gideon RK, Ejegu H, Gatew Y (2022) Extraction and characterization of fiber from the stem of Cyperus papyrus plant. *J Nat Fibers* 20. <https://doi.org/10.1080/15440478.2022.2149661>
 32. Montalvo JG, Von Hoven TM (2008) Review of standard test methods for moisture in lint cotton. *J Cotton Sci* 12:33–47
 33. Gopinath R, Billigraham P, Sathishkumar TP (2022) Characterization studies on new cellulosic fiber extracted from Leucaena leucocephala tree. *J Nat Fibers* 20. <https://doi.org/10.1080/15440478.2022.2157922>
 34. Dutta S, Kim NK, Das R, Bhattacharyya D (2019) Effects of sample orientation on the fire reaction properties of natural fibre composites. *Compos B Eng* 157:195–206. <https://doi.org/10.1016/j.compositesb.2018.08.118>
 35. Creely JJ, Conrad M (1959) Empirical method for estimating the degree of crystallinity of native cellulose using the X-ray diffractometer. *Text Res J* 29:786–794. <https://doi.org/10.1177/00405175590290100>
 36. Rosdi MHHM, Ahad NA, Shahdan D (2022) Comparison on oil and water absorption ability of various natural fiber. *J Phys Conf Ser* 2169. <https://doi.org/10.1088/1742-6596/2169/1/012021>
 37. Weibull W (1951) Wide applicability. *J Appl Mech* 18:293–297
 38. Belaadi A, Amroune S, Seki Y et al (2022) Extraction and characterization of a new lignocellulosic fiber from Yucca treculeana L. leaf as potential reinforcement for industrial biocomposites. *J Nat Fibers* 19:12235–12250. <https://doi.org/10.1080/15440478.2022.2054895>
 39. Khan A, Vijay R, Singaravelu DL et al (2019) Extraction and characterization of natural fiber from Eleusine indica grass as reinforcement of sustainable fiber-reinforced polymer composites. *J Nat Fibers* 18:1742–1750. <https://doi.org/10.1080/15440478.2019.1697993>
 40. Gedik G (2021) Extraction of new natural cellulosic fiber from Trachelospermum jasminoides (star jasmine) and its characterization for textile and composite uses. *Cellulose* 28. <https://doi.org/10.1007/s10570-021-03952-1>
 41. Amutha V, Senthilkumar B (2019) Physical, chemical, thermal, and surface morphological properties of the bark fiber extracted from Acacia concinna plant. *J Nat Fibers* 18:1661–1674. <https://doi.org/10.1080/15440478.2019.1697986>
 42. Manimaran P, Vignesh V, Khan A et al (2022) Extraction and characterization of natural lignocellulosic fibres from Typha angustata grass. *Int J Biol Macromol* 222:1840–1851. <https://doi.org/10.1016/j.ijbiomac.2022.09.273>
 43. Bright BM, Selvi BJ, Abu Hassan S et al (2021) Characterization of natural cellulosic fiber from Cocos nucifera Peduncle for sustainable biocomposites. *J Nat Fibers* 19:9373–9383. <https://doi.org/10.1080/15440478.2021.1982827>
 44. Plant AR, Baye B (2021) Characterization of a new fiber from Cyperus dichrostachus. *J Mater Sci* 10. <https://doi.org/10.4172/2321-6212.10.3.002>
 45. Selvan MTGA, Binoj JS, Moses JTEJ et al (2022) Extraction and characterization of natural cellulosic fiber from fragrant screw pine prop roots as potential reinforcement for polymer composites. *Polym Compos* 43:320–329. <https://doi.org/10.1002/PC.26376>

46. Khan A, Vijay R, Singaravelu DL et al (2020) Extraction and characterization of natural fibers from *Citrullus lanatus* climber. *J Nat Fibers* 19:621–629. <https://doi.org/10.1080/15440478.2020.1758281>
47. Senthamarai kannan P, Sanjay MR, Bhat KS et al (2019) Characterization of natural cellulosic fiber from bark of *Albizia amara*. *J Nat Fibers* 16:1124–1131. <https://doi.org/10.1080/15440478.2018.1453432>
48. Boumediri H, Bezazi A, Garcia G et al (2019) Extraction and characterization of vascular bundle and fiber strand from date palm rachis as potential bio-reinforcement in composite. *Carbohydr Polym* 222:114997. <https://doi.org/10.1016/j.carbpol.2019.114997>
49. Indran S, Divya D, Raja S et al (2022) Physico-chemical, mechanical and morphological characterization of *Furcraea selloa* K. Koch plant leaf fibers—an exploratory investigation. *J Nat Fibers* 20:1–17. <https://doi.org/10.1080/15440478.2022.2146829>
50. Shanmugasundaram N, Rajendran I, Ramkumar T (2018) Characterization of untreated and alkali treated new cellulosic fiber from an Areca palm leaf stalk as potential reinforcement in polymer composites. *Carbohydr Polym* 195:566–575. <https://doi.org/10.1016/j.carbpol.2018.04.127>
51. Mayandi K, Rajini N, Pitchipo P et al (2016) Analysis and extraction and characterization of new natural lignocellulosic fiber *Cyperus pangorei*. *GPAC* 21:175–183. <https://doi.org/10.1080/1023666X.2016.1132064>
52. Vinod A, Vijay R, Singaravelu DL et al (2019) Characterization of untreated and alkali treated natural fibers extracted from the stem of *Catharanthus roseus*. *Mater Res Express* 6:8. <https://doi.org/10.1088/2053-1591/ab22d9>
53. Maache M, Bezazi A, Amroune S et al (2017) Characterization of a novel natural cellulosic fiber from *Juncus effusus* L. *Carbohydr Polym* 171:163–172. <https://doi.org/10.1016/j.carbpol.2017.04.096>
54. Lekrine A, Belaadi A, Makhlof A et al (2022) Structural, thermal, mechanical and physical properties of *Washingtonia filifera* fibres reinforced thermoplastic biocomposites. *Mater Today Commun* 31. <https://doi.org/10.1016/j.mtcomm.2022.103574>
55. Selvaraj M, Akash S, Mylsamy B, Plant D (2023) Characterization of new natural fiber from the stem of *Tithonia diversifolia* plant. *J Nat Fibers* 20. <https://doi.org/10.1080/15440478.2023.2167144>
56. Johnny V, Kuriakose Mani A, Palanisamy S et al (2023) Extraction and physico-chemical characterization of pineapple crown leaf fibers (PCLF). *Fibers* 11. <https://doi.org/10.3390/fib11010005>
57. Bezazi A, Belaadi A, Bourchak M et al (2014) Novel extraction techniques, chemical and mechanical characterisation of *Agave americana* L. natural fibres. *Compos B Eng* 66:194–203. <https://doi.org/10.1016/j.compositesb.2014.05.014>
58. Maria I, Rosa D, Kenny JM et al (2011) Effect of chemical treatments on the mechanical and thermal behaviour of okra (*Abelmoschus esculentus*) fibres. *Compos Sci Technol* 71:246–254. <https://doi.org/10.1016/j.compscitech.2010.11.023>
59. Ganapathy T, Sathiskumar R, Senthamarai kannan P et al (2019) Characterization of raw and alkali treated new natural cellulosic fibres extracted from the aerial roots of banyan tree. *Int J Biol Macromol* 138:573–581. <https://doi.org/10.1016/j.ijbiomac.2019.07.136>
60. Kumar R, Sivaganesan S, Senthamarai kannan P et al (2020) Characterization of new cellulosic fiber from the bark of *Acacia nilotica* L. *Plant J Nat Fibers* 19:199–208. <https://doi.org/10.1080/15440478.2020.1738305>
61. Chakravarthy KS, Madhu SM, Naga Raju JS, Shariff MdJ (2020) Characterization of novel natural cellulosic fiber extracted from the stem of *Cissus vitiginea* plant. *Int J Biol Macromol* 161:1358–1370. <https://doi.org/10.1016/j.ijbiomac.2020.07.230>
62. Belouadah Z, Ati A, Rokbi M (2015) Characterization of new natural cellulosic fiber from *Lygeum spartum* L. *Carbohydr Polym* 134:429–437. <https://doi.org/10.1016/j.carbpol.2015.08.024>
63. Manimaran P, Sanjay MR, Senthamarai kannan P et al (2018) Synthesis and characterization of cellulosic fiber from red banana peduncle as reinforcement for potential applications. *J Nat Fibers* 16:768–780. <https://doi.org/10.1080/15440478.2018.1434851>
64. Manimaran P, Saravanan SP, Sanjay MR et al (2019) Characterization of new cellulosic fiber: *Dracaena reflexa* as a reinforcement for polymer composite structures. *J Mater Res Technol* 8:1952–1963. <https://doi.org/10.1016/j.jmrt.2018.12.015>
65. Ichazo M, Kaiser D, Albano C, Gonza J (1999) Thermal stability of blends of polyolefins and sisal fiber. *Polym Degrad Stab* 66:179–190
66. Jabli M, Tka N, Ramzi K, Saleh TA (2018) Physicochemical characteristics and dyeing properties of lignin-cellulosic fibers derived from *Nerium oleander*. *J Mol Liq* 249:1138–1144. <https://doi.org/10.1016/j.molliq.2017.11.126>
67. Eyupoglu S (2020) Characterization of new cellulosic fibers obtained from *Zingiber officinale*. *J Nat Fibers* 19:1287–1296. <https://doi.org/10.1080/15440478.2020.1764452>
68. Selvaraj M, Chapagain P, Mylsamy B (2022) Characterization studies on new natural cellulosic fiber extracted from the stem of *Ageratina adenophora* plant. *J Nat Fibers* 20. <https://doi.org/10.1080/15440478.2022.2156019>
69. Soltani P, Taban E, Faridan M et al (2020) Experimental and computational investigation of sound absorption performance of sustainable porous material: *Yucca gloriosa* fiber. *Appl Acoust* 157. <https://doi.org/10.1016/j.apacoust.2019.106999>
70. Sikame Tagne NR, Njeugna E, Fogue M, et al (2014) Study of water absorption in raffia *vinifera* fibres from Bandjoun, Cameroon. *Sci World J* 2014. <https://doi.org/10.1155/2014/912380>
71. Peleg M (1988) An empirical model for the description moisture sorption curves. *J Food Sci* 53:1216–1217. <https://doi.org/10.1111/j.1365-2621.1988.tb13565.x>
72. Mbou ET, Njeugna E, Kemajou A et al (2017) Modelling of the water absorption kinetics and determination of the water diffusion coefficient in the pith of raffia *vinifera* of Bandjoun, Cameroon. *Adv Mater Sci Eng* 2017. <https://doi.org/10.1155/2017/1953087>

Publisher's Note Springer Nature remains neutral with regard to jurisdictional claims in published maps and institutional affiliations.

Springer Nature or its licensor (e.g. a society or other partner) holds exclusive rights to this article under a publishing agreement with the author(s) or other rightsholder(s); author self-archiving of the accepted manuscript version of this article is solely governed by the terms of such publishing agreement and applicable law.